

**SEASONAL VARIATION IN MARTIAN WATER ICE CLOUD PARTICLE SIZE.** S.D. Guzewich<sup>1</sup> (scott.d.guzewich@nasa.gov) and M.D. Smith<sup>1</sup>, NASA Goddard Space Flight Center, Greenbelt, MD.

**Introduction:** Scattering and absorption of solar radiation by water ice particles is dependent on the size of those particles. Given the importance of water ice clouds in the martian general circulation and water cycle [e.g., 1], understanding the microphysical aspects of water ice particles is critical. As microphysical properties are often utilized in general circulation models as “tuning parameters”, observations of martian water ice cloud particles can help models move toward improved self-consistency.

**Methodology:** We utilize the complete record of limb-viewing observations by the Compact Reconnaissance Imaging Spectrometer for Mars (CRISM). These observations were collected when the Mars Reconnaissance Orbiter (MRO) was pitched to allow CRISM to scan the limb of the planet rather than the surface as normal. These observations required the CRISM cryo-cooler, which has since failed well beyond its design lifetime. CRISM’s visible and near-infrared channels are utilized to retrieve water ice (and dust) extinction mixing ratios, particle effective radii, and Lambert surface albedo at each wavelength used in the retrieval. Retrievals are calculated in 0.4 scale height-thick layers from approximately 0.2 to 6.6 scale heights above the surface. Additional details of the retrieval are presented in [2], [3], and [4].

In total, 922 successful vertical profiles are retrieved. As CRISM relies on sunlight scattered within the atmosphere and surface, all observations are taken at the ~1500 local time of the MRO orbit. Due to the scheduling cadence of the observations, most fall within 2 distinct longitude bands near 80-100°E and 270-310°E. Due to the timing variation of the observations across several Mars years, interannual variations (if they exist) were not distinguishable and all years were combined in the analysis.

**Results:** Figures 1 and 2 show the evolution of water ice mixing ratio and effective radius in the martian tropics throughout the year. Tropical clouds exhibit a strong sorting of particle size with height throughout the year with small particles at lower altitudes and smaller particles at higher altitudes.

Cloud mixing ratios peak during the aphelion cloud belt season in the northern spring and summer ( $L_s = 30-180^\circ$ ) and the altitude of maximum mixing ratio increases throughout the year before decreasing again after northern summer solstice ( $L_s = 270^\circ$ ). The largest cloud particles (2.5-3  $\mu\text{m}$  in radius) follow this pattern and rise from below 20 km altitude at  $L_s = 90^\circ$

to 35-40 km at  $L_s = 240^\circ$ ). At the center of the cloud layer (the seasonally-varying altitude with the highest ice mixing ratio), the ice particle size varies by 0.7  $\mu\text{m}$  with a mean value near 1.9  $\mu\text{m}$ .

The seasonal variation in ice particle size is clearest in the 30-45 km altitude range in the tropics (Figure 2). In this altitude range, ice particle size varies by 1.5  $\mu\text{m}$  through the year with a minimum near  $L_s = 60^\circ$  and a maximum near  $L_s = 240^\circ$ .

While the seasonal cycles of water ice mixing ratio and particle size are similar, they have some notable differences as well which suggests different, albeit linked, processes control these two aspects of martian tropical clouds.

The addition of >500 limb-viewing profiles in [2] compared to [3] allows a more complete understanding of northern hemisphere polar clouds as well. Whereas [3] noted a relatively uniform vertical profile of ice particle size near 1.5  $\mu\text{m}$ , our more complete record shows that the ice particle size profile is steeply sloped with height during early northern autumn ( $L_s = 180-210^\circ$ ) and transitions to one that is more uniform with height after the winter solstice ( $L_s = 330-30^\circ$ ).

#### References:

- [1] Steele, L.J., et al. (2014) *GRL*, 41, 4471-4478.
- [2] Guzewich, S.D. and M.D. Smith (2019) *JGR*, 124, 636-643.
- [3] Guzewich, S.D. et al. (2014) *JGR*, 119, 2694-2708.
- [4] Smith, M.D. et al. (2013) *JGR*, 118, 321-334.

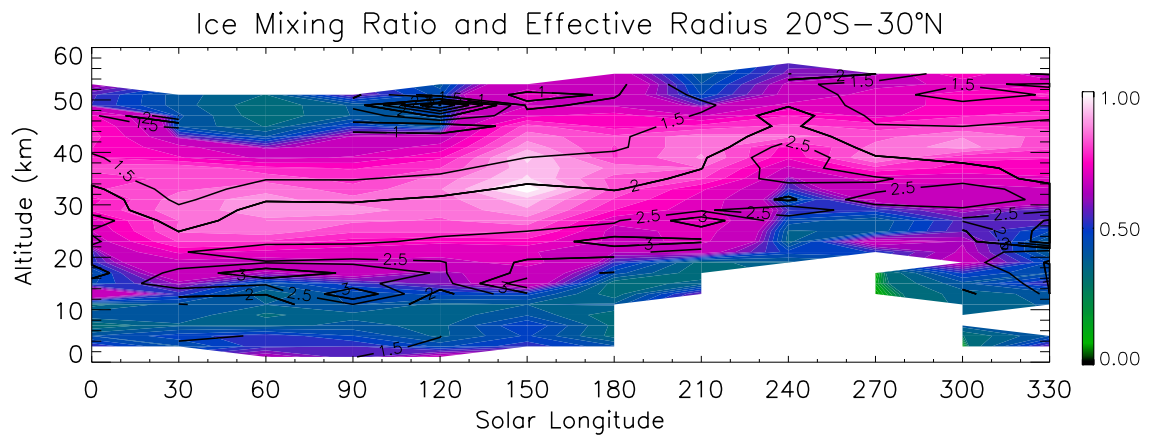


Figure 1. Zonal-averaged water ice mixing ratio ( $\Delta\tau/\Delta m_b$ , color shading) and effective radius ( $\mu\text{m}$ , contours).

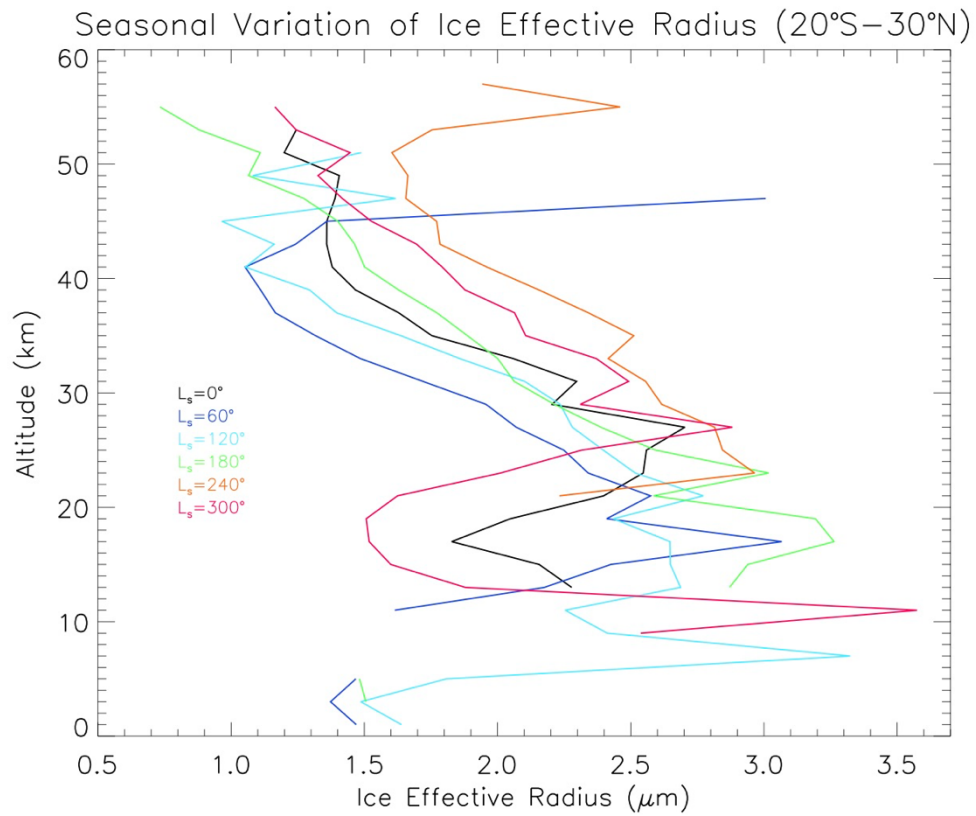


Figure 2. Zonal-averaged water ice effective radius binned by 60° of solar longitude.